

## Soot Oxidation during the Burn-out Phase of Diesel Combustion in a Small-Bore Optical Engine

L. Rao<sup>1</sup>, R. Zhang<sup>1</sup>, H.C. Su<sup>1</sup>, and S. Kook<sup>1,\*</sup>

<sup>1</sup>School of Mechanical and Manufacturing Engineering  
The University of New South Wales, Sydney, NSW 2052, Australia

### Abstract

Diesel engines, while being treated as the most efficient type of combustion engines for mobile applications, are also suffered from the problematic soot emissions. For past decades, under the goal of impairing such sooting behaviour, a great quality of study has been done with respect to the oxidation process of in-cylinder soot, which is dominated by O<sub>2</sub> molecules and OH radicals. However, little is understood about left-over soot observed in the late-cycle burn-out phase, which eventually would be emitted to the environment. This experimental study performs planar laser diagnostic techniques to visualise spatial and temporal evolution of soot and OH radicals during this burn-out phase in a light duty optically accessible diesel engine. In addition to the main injection, a small amount of fuel is added upon the completion of the main combustion event (i.e. after-injection), which is previously proven to be effective in reducing engine-out soot due to the promotion of the late-cycle soot oxidation. The results show that, with the introduction of the after-injection, new OH radicals are produced coherent with the increased in-cylinder bulk gas temperature near the main-injection induced soot pockets. As a result, the oxidation of in-cylinder soot particles is accelerated.

### Introduction

Diesel engines have enjoyed an immense popularity in the global market owing to their remarkable performance in fuel economy and high torque output. However, as a trade-off, engine-out soot particles have been known to adversely affect both the environment and human health. To resolve this emission issue and to meet the ever-tightening regulations on it, a large amount of technologies in terms of in-cylinder reduction and exhaust after treatment have been developed. For instance, diesel particle filter (DPF), as one of the most widely used exhaust after-treatment, is an effective tool in reducing engine-out soot emission. However, with its costly system, sacrifices made in fuel economy, and the periodical regeneration process that has found to cause a low filtering efficiency period [1], in-cylinder reduction is still an effective way to directly reduce combustion-generated soot. Benefiting from the invention of common rail injection system, a stable meanwhile more flexible control of diesel injection is achieved. As a result, a multiple injection strategy has been put into practice and intensively studied as a method that can promote diesel combustion in terms of thermal efficiency and emission control.

Among all multiple injection strategies, after injection, or in some cases been referred as close-coupled post-injection, has been proven to be effective in reducing soot emission by a number of previous studies [2-5]. It is well known that enhanced mixing and increased in-cylinder temperature are two main factors controlling the oxidation as well as formation rate of in-

cylinder soot particles [5]. In this regard, the interaction between the main and after injection causes increased oxidation rate as the fuel jet craves out the main combustion soot cloud and increase the mixing [2]. The after-injection fuel jet also drives the main-combustion soot to the squish area where local temperature is higher and thereby stimulating the soot oxidation [3].

The present study aims to visualise the in-cylinder soot distributions under the influence of after-injection executed in the late-cycle burn out phase of diesel combustion so that its impact on soot oxidation is better understood. Various imaging diagnostics have been performed in an optically accessible diesel engine, including planar laser induced incandescence (PLII), OH planar laser induced fluorescence (OH-PLIF) and electronically excited OH (OH\*) chemiluminescence. With three different elevations of the laser sheet below the cylinder head, both the horizontal and the vertical distributions of in-cylinder soot and OH radicals have been imaged. The pressure measurement has also been conducted simultaneously to evaluate the in-cylinder conditions.

### Methodology

#### Engine Specification and Operating Conditions

The imaging diagnostics was performed in a single-cylinder, light-duty optical diesel engine modified from a conventional 2-litre, four-cylinder diesel engine. The simplified engine configuration is shown in figure 1 and the engine specifications as well as operating conditions are summarised in table 1. The engine has a displacement volume of 497.5 cm<sup>3</sup> with 83 mm bore and 92 mm stroke, a geometric compression ratio of 15.5, and a swirl ratio of 1.4. Throughout the experiments, the engine speed was held constant at 1200 rpm.

The engine was kept with the cylinder head and liner wall temperature of 363 K and an intake air temperature of 303 K to simulate warmed-up and thermally stable operating conditions. A piezoelectric transducer (Kistler 6056A1) is installed next to the centrally mounted common-rail fuel injector (Bosch CP3) on the conventional flat engine head between two pairs of intake and exhaust valves. The original injector nozzle had evenly-spaced 7 holes with 150° included angle but in the present study, only one hole was left open. The nozzle hole size is 134 μm in diameter (nominal). The common-rail pressure was fixed at 100 MPa. Methyl decanoate was selected as a diagnostic fuel due to its very low sooting property [6] and thereby avoiding the beam attenuation problem [7]. The main injection timing was fixed at 11°CA aTDC with duration 1.2 ms meanwhile a short after injection at 25°CA aTDC with duration of 0.3 ms was executed to affect the burn-out phase of the combustion event.

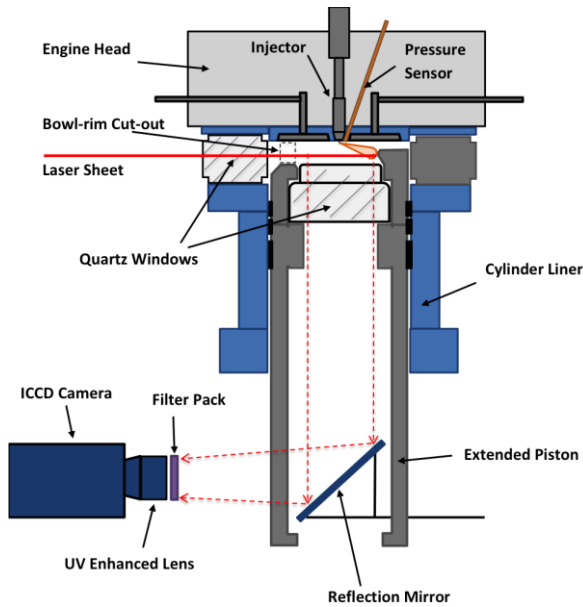


Figure 1 Schematic diagram of the optical diesel engine and laser-based imaging setup.

Table 1 Engine specifications and operating conditions.

Displacement (single-cylinder)	497.5 cm <sup>3</sup>
Bore	83 mm
Stroke	92 mm
Compression ratio	15.5 (geometric)
Engine speed	1200 rpm
Swirl ratio	1.4
Wall (coolant) temperature	363 K
Intake air temperature	303 K
Injector type	Common-rail (Bosch CP3)
Number of holes	1
Nozzle type	Hydro-grounded, K1.5/0.86
Nozzle diameter	134 $\mu$ m
Included angle	150°
Rail pressure	100 MPa
Fuel	Methyl Decanoate
Lower heating value	37.7 MJ/kg
Cetane Number	52
Main injected fuel mass per hole	11.5 mg
Main injection signal duration	1.2 ms
Main injection signal timing	11°CA bTDC
After injection signal timing	25°CA aTDC
After injection fuel mass per hole	2.9 mg
After injection signal duration	0.3 ms

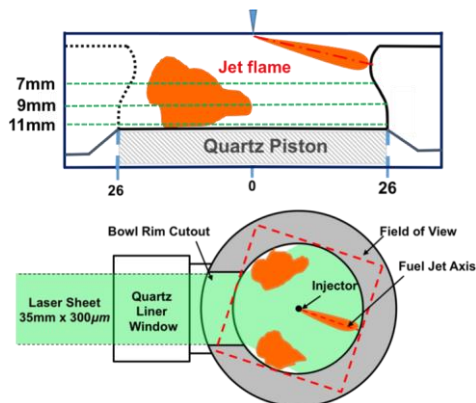


Figure 2 Illustration of the laser sheet positions with respect to the piston bowl and fuel jet in the side view (top) and top view (bottom).

## Optical/Laser-based Imaging Diagnostics Setup

As shown in figure 1, the optical access of the engine is achieved through two quartz windows on the extended piston top and the liner window. The void section of the extended piston design enables the installation of a 45-degree reflection mirror, which allows an intensified charge-coupled device (ICCD) camera (LaVision NanoStar) equipped with a 105-mm f/4.5 UV-enhanced lens to capture the bottom view of the combustion chamber.

Figure 2 shows how the laser sheet was inserted into the combustion chamber. Three horizontal planes were visualised at 7, 9 and 11 mm below the cylinder head. In the present study, a Rhodamine-6G filled dye laser and an Nd:YAG laser are used for generating laser pulses for two types of laser diagnostic techniques. The two lasers were firstly used to generate 284 nm beam for planar laser induced fluorescence of OH radicals (OH-PLIF). The 284 nm laser beam was generated by introducing the frequency-doubled 532 nm beam from the Nd:YAG laser into the dye laser. To isolate the OH-PLIF signal, a filter pack comprising a 300-nm band pass filter (40-nm FWHM), two WG-305 long pass filters and two WG-295 long pass filter were used. It was noted that the interference signals (e.g. fuel-PLIF) are minimal in the late-cylinder burn-out stage with this set of filters [8]. In addition to OH-PLIF, electronically-excited OH (OH\*) chemiluminescence imaging was also performed to provide complimentary information of the development of high-temperature reaction zone. For the same engine operating conditions, planar laser-induced incandescence (PLII) imaging was also performed for the visualisation of in-cylinder soot. For PLII imaging, a 1064-nm laser beam generated by the Nd:YAG laser was directed into the combustion chamber to heat up in-cylinder soot particles for strong incandescence signals. The laser pulse is highly energised to a level above 0.4 J/cm<sup>2</sup> to exceed the laser fluence threshold. To capture the soot incandescence signals below 500 nm [9], a 450-nm short-pass filter together with a 430-nm band-pass filter were used. This was to minimise interference from other signals (e.g. heated C<sub>2</sub> [8]).

## Results and Discussion

The ensemble-averaged traces of in-cylinder pressure and apparent heat release rate (aHRR) together with the estimated bulk gas “in-cylinder” temperature are shown in figure 3. For a comparison purpose, the main-only injection data are also plotted using a black line. Shortly after the start of injection at 25°CA aTDC, a slight drop in aHRR can be spotted, indicating a short ignition delay period for the after injection. This is then followed by a distinct spike in aHRR as an indicator of a second combustion event. The in-cylinder pressure for the main+after injection case rises from the reference main-only injection case, which starts from approximately 30°CA aTDC. The pressure deviation is highlighted in the insert plot for the close-up view of this crank angle range. The influence of the after injection on in-cylinder conditions is also observed in the estimated in-cylinder temperature, which is roughly 50 K higher at any fixed crank angle compared with the main-only injection case.

Figure 4 shows OH\* chemiluminescence images (top row) and combined OH-PLIF and PLII images during this late-cycle burn-out stage. The planar laser images are shown for three different elevations below the cylinder head. It should be noted that the images presented in figure 4 are a selected image out of 20 images from different engine cycles. These are the most representative image of a given timing that resembles the ensemble-averaged image the most, which was evaluated using a correlation coefficient factor-based method [8].

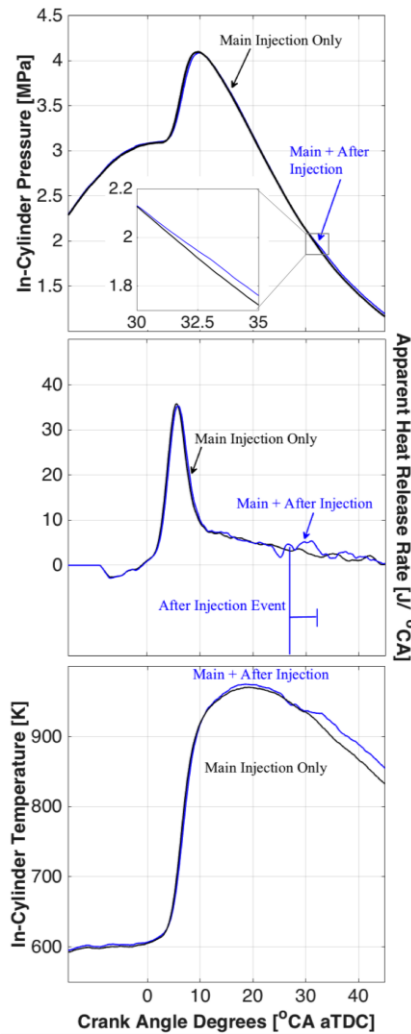


Figure 3 Ensemble-averaged in-cylinder traces, apparent heat release traces and in-cylinder bulk gas temperature traces for the main-only injection and main + after-injection cases.

The OH\* chemiluminescence images exhibit a gradual decrease of signals during this burn-out stage. From this line-of-sight integrated image, no clear sign of the after-injection-induced combustion can be spotted. However, OH-PLIF signals at 30°CA aTDC suggests a line of fluorescence signals along the fuel jet axis (highlighted by a red dashed box) at 7 mm below the cylinder head. This signal can be recognised as fuel fluorescence signals of the after-injection fuel jet. This together with the in-cylinder conditions (figure 3) confirms the high-temperature reaction induced by the after-injection despite its very small mass (2.9 mg). The absence of OH\* chemiluminescence signal could be due to the heat release for only a short period of time and insufficient reaction temperature to induce electronically-excited OH radicals.

In contrast to the OH\* chemiluminescence images, the combined OH-PLIF and PLII images clearly suggest the effects of after-injection. It is understood that the tested after-injection did not produce any additional soot. However, the spatial development of OH-PLIF signals shows an increase in OH coverage (especially on the 9-mm plane) from 27.5 to 30°CA aTDC. This expanded coverage of OH-PLIF signals implies that new OH radicals are produced due to the after-injection combustion, which is consistent with the increase in in-cylinder temperature starting to occur at 30°CA aTDC (Fig. 3). With the increased OH radicals and higher in-cylinder bulk gas temperature, the oxidation rate of

in-cylinder soot particles would increase. This is indeed well supported by PLII images. For example, slightly after the increase in OH radicals, the PLII signals on all three planes quickly fade away indicating the disappearance of in-cylinder soot due to oxidation.

To further analyse the observed trend and rule out the question on the effect of cycle-to-cycle variations, figure 5 shows two selected PLII images obtained at 9 mm below the cylinder and at 30 and 32.5°CA aTDC during which the increased OH-PLIF signals and the rapid disappearance of PLII signals are noticed (figure 4). For each case, six raw images are presented, which confirms that the disappearance of soot signals is real, not a result of cyclic variations.

## Conclusion

This study applies optical/laser-based imaging diagnostics of late-cycle diesel combustion occurring in a single-cylinder optical diesel engine with an emphasis on the in-cylinder distribution of soot and OH radicals. With additional injection of a small amount of fuel after the main combustion event (i.e. after injection), it is apparent that the after-injection triggers a second combustion apart from the main combustion that increases in-cylinder pressure and temperature. The after-injection does not produce additional soot but new OH radicals during the late-cycle burn-out phase of the main combustion, which promote the oxidation rate of in-cylinder soot of the main combustion.

## References

- [1] Di Iorio, S., Beatrice, C., Guido, C., Del Giacomo, N., Napolitano, P., Vassallo, A., Analysis of Particle Mass and Size Emissions from a Catalyzed Diesel Particulate Filter during Regeneration by Means of Actual Injection Strategies in Light Duty Engines, *SAE Int. J. Engines*, 2011, 2510-2518.
- [2] O'Connor, J., Musculus, M., In-Cylinder Mechanisms of Soot Reduction by Close-Coupled Post-Injections as Revealed by Imaging of Soot Luminosity and Planar Laser-Induced Soot Incandescence in a Heavy-Duty Diesel Engine, *SAE Int. J. Engines*, 2014, 2014-01-1225.
- [3] Hotta, Y., Inayoshi, M., Nakakita, K., Fujiwara, K., Sakata, I., Achieving Lower Exhaust Emissions and Better Performance in an HSDI Diesel Engine with Multiple Injection, *SAE Technical Paper*, 2005, 2005-01-0928.
- [4] Desantes, J., Arrègle, J., López, J., García, A., A Comprehensive Study of Diesel Combustion and Emissions with Post-Injection, *SAE Technical Paper*, 2007, 2007-01-0915.
- [5] Yue, Z., Hessel, R., Reitz, R., CFD Study of Soot Reduction Mechanisms of Post-Injection in Spray Combustion, *SAE Technical Paper*, 2015, 2015-01-0794.
- [6] Cheng, A.S., Dumitrescu, C.E., Mueller, C.J., Investigation of Methyl Decanoate Combustion in an Optical Direct-Injection Diesel Engine, *Energy and Fuels*, 2014, 7689-7700.
- [7] Dec, J., zur Loye, A., Siebers, D., Soot Distribution in a D.I. Diesel Engine Using 2-D Laser-Induced Incandescence Imaging, *SAE Technical Paper*, 1991, 910224.
- [8] Le, M.K., Zhang, R., Rao, L., Kook, S., Hawkes, E.R., The Development of Hydroxyl and Soot in a Methyl Decanoate-Fuelled Automotive-Size Optical Diesel Engine, *Fuel*, 166, 2016, 320 – 332.
- [9] Dec, J., Soot Distribution in a D.I. Diesel Engine Using 2-D Imaging of Laser-Induced Incandescence, Elastic Scattering, and Flame Luminosity, *SAE Technical Paper*, 1992, 920115.

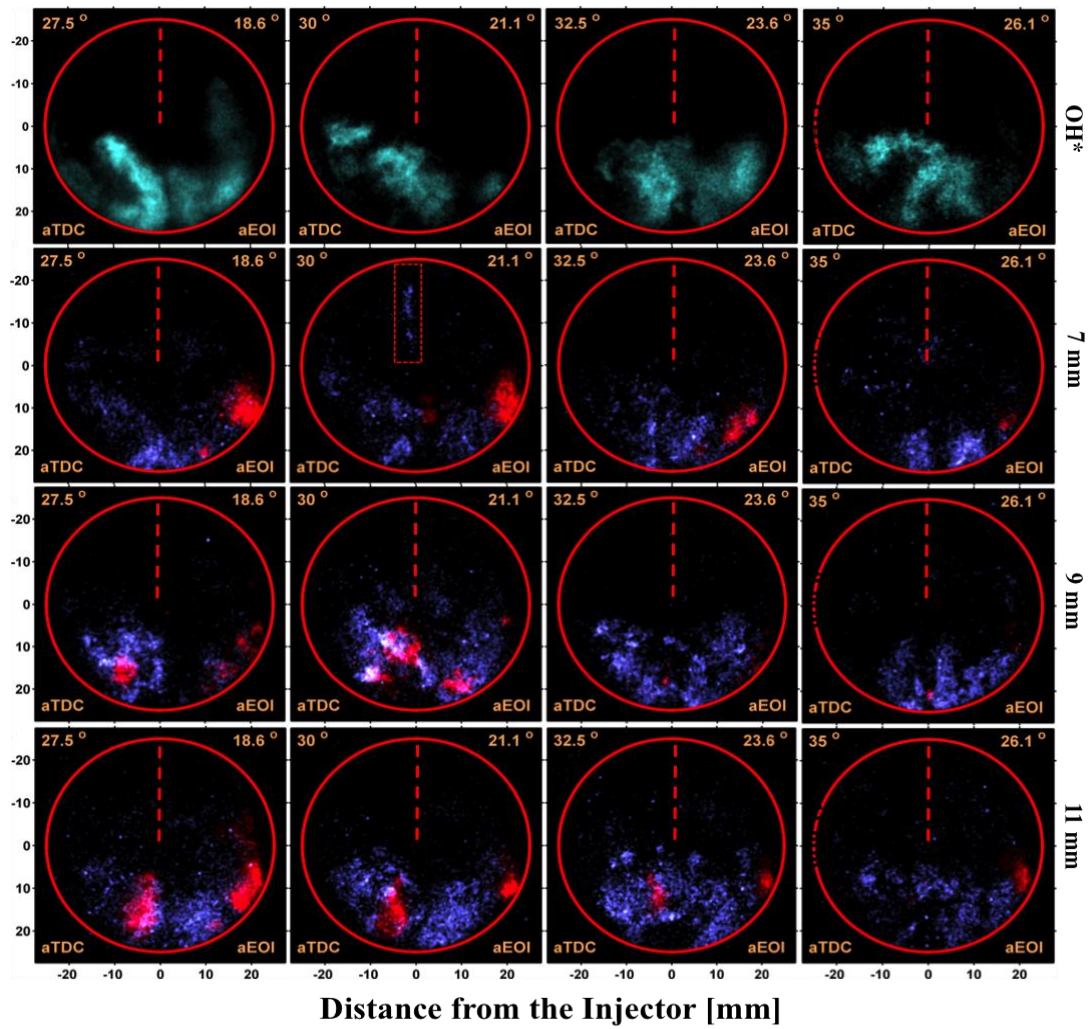


Figure 4 Images of OH\*, OH-PLIF and PLII during the late-cycle, burn-out phase of diesel combustion. On the top-left corner, the crank angle ( $^{\circ}$ CA aTDC) of the imaging timing is denoted. The corresponding crank angle after the end of main injection is also shown at the top-right of each image.

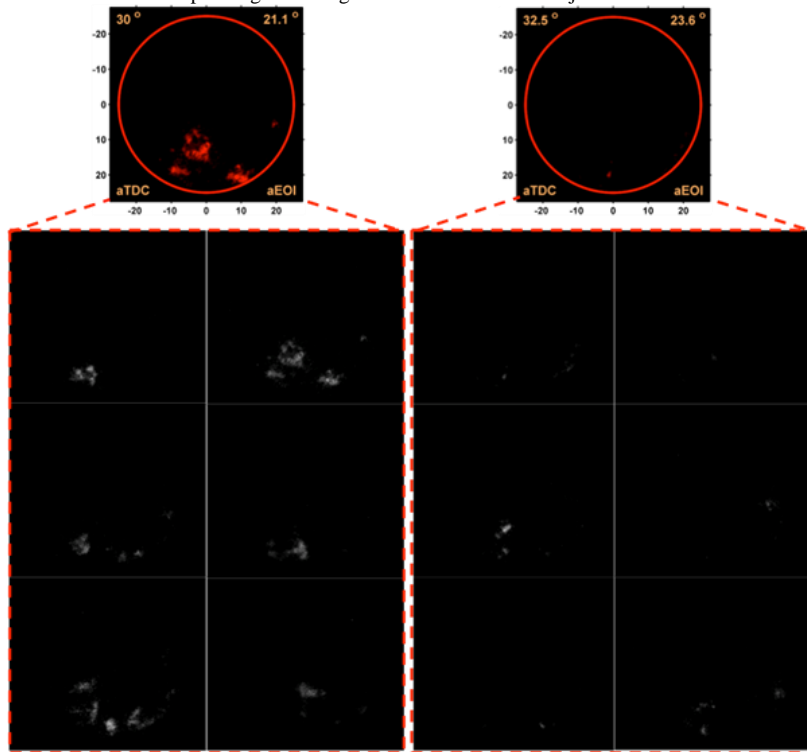


Figure 5 The selected PLII images at 30 and 32.5  $^{\circ}$ CA aTDC (top) and six raw images of each crank angle (bottom)